Simulation of a hydrogen production and purification system for a PEM fuel-cell using bioethanol as raw material

Pablo Giunta [a], Carlos Mosquera [b], Norma Amadeo [a], Miguel Laborde [a,*]

[a] *Facultad de Ingeniería, Universidad de Buenos Aires, Laboratorio de Procesos Catalíticos, Pabellón de Industrias, Ciudad Universitaria, 1428 Buenos Aires, Argentina*
[b] *Facultad de Ingeniería, Universidad de Buenos Aires, Departamento de Física, 1063 Buenos Aires, Argentina*

Abstract

A process to produce "fuel-cell grade" hydrogen from ethanol steam reforming is analyzed from a thermodynamic point of view. The hydrogen purification process consists of WGS and COPROX reactors. Equations to evaluate the efficiency of the system, including the fuel cell, are presented. A heat exchange network is proposed in order to improve the exploitation of the available power. The effect of key variables such as the reformer temperature and the ethanol/water molar feed ratio on the fuel-cell efficiency is discussed. Results show that it is feasible to carry out the energy integration of the hydrogen catalytic production and purification—PEM fuel-cell system, using ethanol as raw material. The technology of "fuel-cell grade" hydrogen production using ethanol as raw material is a very attractive alternative to those technologies based in fossil fuels.
© 2006 Elsevier B.V. All rights reserved.

Keywords: Hydrogen production and purification; Bioethanol; PEM fuel-cells

1. Introduction

Fuel cells and hydrogen as a fuel can be a solution in the development of zero emission vehicles [1,2]. In addition, hydrogen is the future fuel, basically since its combustion only produces water. Nevertheless, some considerations must be made about this asseveration. Firstly, if the combustion of hydrogen is performed with air, nitrogen oxides will also be produced. Second, hydrogen is not free in Nature; this element is present in hydrocarbons and in the water. Energy has to be consumed in order to separate it from carbon (hydrocarbons) or from oxygen (water). When hydrogen is obtained from water the process used is the electrolysis, which consumes a significant amount of energy. Only if this energy is produced from renewable sources such as solar or wind energy, it can be said that hydrogen is obtained using a non-pollutant process. On the other hand, when hydrogen is obtained from hydrocarbon or alcohol steam reforming, carbon oxides are produced as well. Thus, the qualification of "clean" fuel is only true when the raw material is biomass, which consumes CO_2 during its growth.

Ethanol presents several advantages related to natural availability, storage and handling safety. It can be produced renewably from several biomass sources, including energy plants, waste materials from agro industries or forestry residue materials, organic fraction of municipal solid waste, etc. Besides the bioethanol-to-hydrogen system has the significant advantage of being nearly CO_2 neutral, since the carbon dioxide produced is consumed for biomass growth, thus offering a nearly closed carbon cycle. In summary, among the various processes and primary fuels that have been proposed in the production of hydrogen for fuel-cell applications, steam reforming of ethanol is the most attractive [3–8].

The new application of H_2 as a feed for fuel cells for mobile sources (PEM) requires that the anode inlet gas has a CO concentration lower than 20 ppm. Otherwise, the anode is poisoned and the cell efficiency abruptly drops. Hence, if H_2 is produced from hydrocarbons or alcohols, purification is required in order to reduce the CO levels to fuel-cell requirements. So far, the most technologically feasible purification train consists of two water gas shift converters (WGS) and a latter step of remaining CO elimination (COPROX reactor) [9].

* Corresponding author. Tel.: +5411 4576 3240; fax: +5411 4576 3241.
  E-mail address: miguel@di.fcen.uba.ar (M. Laborde).

In this work, a hydrogen production process from ethanol steam reforming is analyzed from a thermodynamic point of view. Equations to evaluate the efficiency of the system, including the fuel cell, are presented. A heat exchange network is proposed in order to improve the exploitation of the available heat. The effect of key variables such as the reformer temperature and the ethanol/water molar feed ratio on the fuel-cell efficiency is discussed.
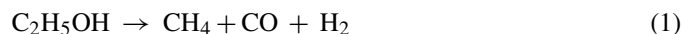
2. System definition

2.1. System of reactors

The process involves three stages:

- Ethanol steam reformer (ESR).
- Water gas shift reactor (WGS).
- CO preferential oxidation reactor (COPROX).

ESR can be modelled using the following equations [3]:

$$C_2H_5OH \rightarrow CH_4 + CO + H_2 \tag{1}$$

$$CO + H_2O \rightleftharpoons CO_2 + H_2 \tag{2}$$

$$CH_4 + H_2O \rightleftharpoons CO + 3H_2 \tag{3}$$

Reaction (1) is very fast and it can be considered complete due to the high value of its equilibrium constant at the operating temperatures considered in the present work [8]; the other two reactions reach equilibrium. In addition, reactions (1) and (3) are endothermic and the reaction (2) (WGS) is exothermic. The whole reaction system is endothermic and the reactor operates, depending on the catalyst activity and the ethanol/water molar ratio, at temperatures ranging 550–800 °C. Nickel or noble metals such as Rhodium and Platinum are proposed as catalysts [3–6,10–12].

In the WGS reactor the only reaction occurring is reaction (2):

$$CO + H_2O \rightleftharpoons CO_2 + H_2.$$
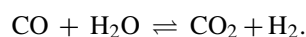
It can be seen that CO is consumed and additional hydrogen is produced. Since this is an exothermic reaction, low temperatures favour the equilibrium. Nevertheless from a kinetic point of view low temperatures are not convenient. Both aspects shall be taken into account to design the reactor. In this sense, two fixed bed catalytic reactors with a heat exchange between them are employed. Both reactors operate at the same inlet temperature (180 °C) and use the same Cu/Zn/Ba/Al₂O₃ catalyst. At these low temperatures copper is the most adequate catalyst [13–17].

Before entering the COPROX reactor, the WGS reactor outlet is mixed with oxygen (or air). In the COPROX reactor, the remaining CO is oxidized to CO₂, but hydrogen is also oxidized:

$$CO + \tfrac{1}{2}O_2 \rightarrow CO_2 \tag{4}$$

$$H_2 + \tfrac{1}{2}O_2 \rightarrow H_2O \tag{5}$$

Reaction (5) must be avoided as much as possible since hydrogen is consumed. Nevertheless, this reaction is thermo-dynamically favoured and besides hydrogen concentration in the mixture entering the reactor is clearly higher than CO concentration. For these reasons, the catalyst shall be highly selective to reaction (4). Two types of catalyst are used: noble metals (Pt and recently Au) and Cu/CeO₂. As both reactions are highly exothermic, an undesirable temperature increase could occur. Hence the reactor is divided into three fixed beds with a heat exchange between them. At the outlet of this reactor CO concentration in the hydrogen-rich flow shall be less than 20 ppm [18–20].

With respect to the heat exchange, adiabatic operation for WGS and COPROX reactors is assumed, while isothermal operation is assumed for the ESR. This is the only reactor which consumes energy due to the endothermic characteristic of the reaction set. There is also heat consumption for feed evaporation, prior to entering the reactor.

2.2. Energy integration

The following variables were taken into consideration:

- Operating pressures.
- Operating temperatures.
- Hot and cold sources.
- Ethanol/water ratio in the ESR feed.
- Temperature approach in the exchanges.

It must be noted that flows are not considered since this is a thermodynamic analysis. Instead, a molar flow basis of 1 kmol h^{-1} is employed. Specifications about these variables will be discussed below.

2.2.1. Operating pressures

As the fuel cell operates at 4.5 atm, pumps and compressors shall be considered. Pressure affects ethanol steam reaction since the total mole number changes due to the reaction: if pressure increases, the conversion in this reactor (ESR) decreases (anyway, the compression will be upstream from the ESR). Pressure does not affect the WGSR since there is no change of the total mole number by the reaction. The COPROX reactor is not affected either since both reactions – (4) and (5) – can be considered irreversible.

2.2.2. Operating temperatures

The fuel cell works at 80–100 °C. The ESR can operate at 550–800 °C. From a constructive point of view, it would be desirable that the ESR worked at lower temperatures, but methane production increases when temperature decreases [5,11]. It must be noted that the higher the methane production is, the lower hydrogen yield will be, since each mole of methane contains two moles of hydrogen. On the contrary, if the ERS operates at high temperatures, the heat consumed by this reactor will be higher, and so will be the stream fraction burned for this purpose (see Section 2.2.8).

WGSR operates between 180 and 250 °C; higher temperatures cause the deactivation of the copper catalyst by sintering. Although at lower temperatures the catalyst is not active [14,16,17], temperatures near 160 °C were allowed.

The lowest temperature at which any COPROX reactor can operate is that of water condensation temperature (about 130 °C at 5 atm) [18–20]. As this reaction is highly exothermic two precautions must be taken into account to avoid high temperatures: (1) the possibility of an undesirable temperature raise and (2) the need to cool the effluent prior to entering the fuel cell.

2.2.3. Hot and cold sources

A hot source is needed to sustain the reaction occurring in the ESR. Similarly, a cold source is needed to reject heat from the PEM fuel-cell feed.

The hot source used is a process stream at high temperature (an internal source of heat). When this source of heat is not at a proper thermal level, a portion of a stream can be combusted in a burner in order to obtain a hot exhaust gas. The burner can be fed by: (a) ethanol, (b) synthesis gas or (c) hydrogen-rich stream. Two new variables shall be considered: the air/fuel ratio and the process stream not burned. The efficiency of the system decreases when the burned fraction increases (see efficiency definition).

In the same way, when a cold source is not at a proper thermal level, the cold source employed can be a cold utility not specified, but capable of removing any amount of heat (e.g. atmospheric air).

It must be noted that when an internal source is employed, it shall not be considered as heat exchanged in Eq. (6).

2.2.4. Feed ethanol/water ratio

Kinetic studies claim that a high ethanol/water ratio in the feed improves the conversion in ESR and WGSR. This ratio does not affect the performance of COPROX reactors [17,18]. Nevertheless, water evaporation consumes a significant amount of heat. Then, if this ratio increases, the system available power decreases because a higher process fraction will have to be burned. Hence, there is a trade-off between the hydrogen production and the heat consumed in water evaporation.

2.2.5. Air/CO ratio in COPROX stage

In this stage both CO and H_2 are oxidized. A lack of air can provoke a wrong operation of the reactor since the CO concentration will not reach the specified value (20 ppm). On the contrary, an excess of air can produce an excessive oxidation of hydrogen reducing its yield [18–20]. In addition, an excess of air increases the electric energy consumption in the compressor. Then there is a trade-off between high and low air/CO ratios.

2.2.6. Temperature approach in the heat exchangers

In order to reduce the heat exchangers size, temperature differences must be as high as possible. This is a relevant
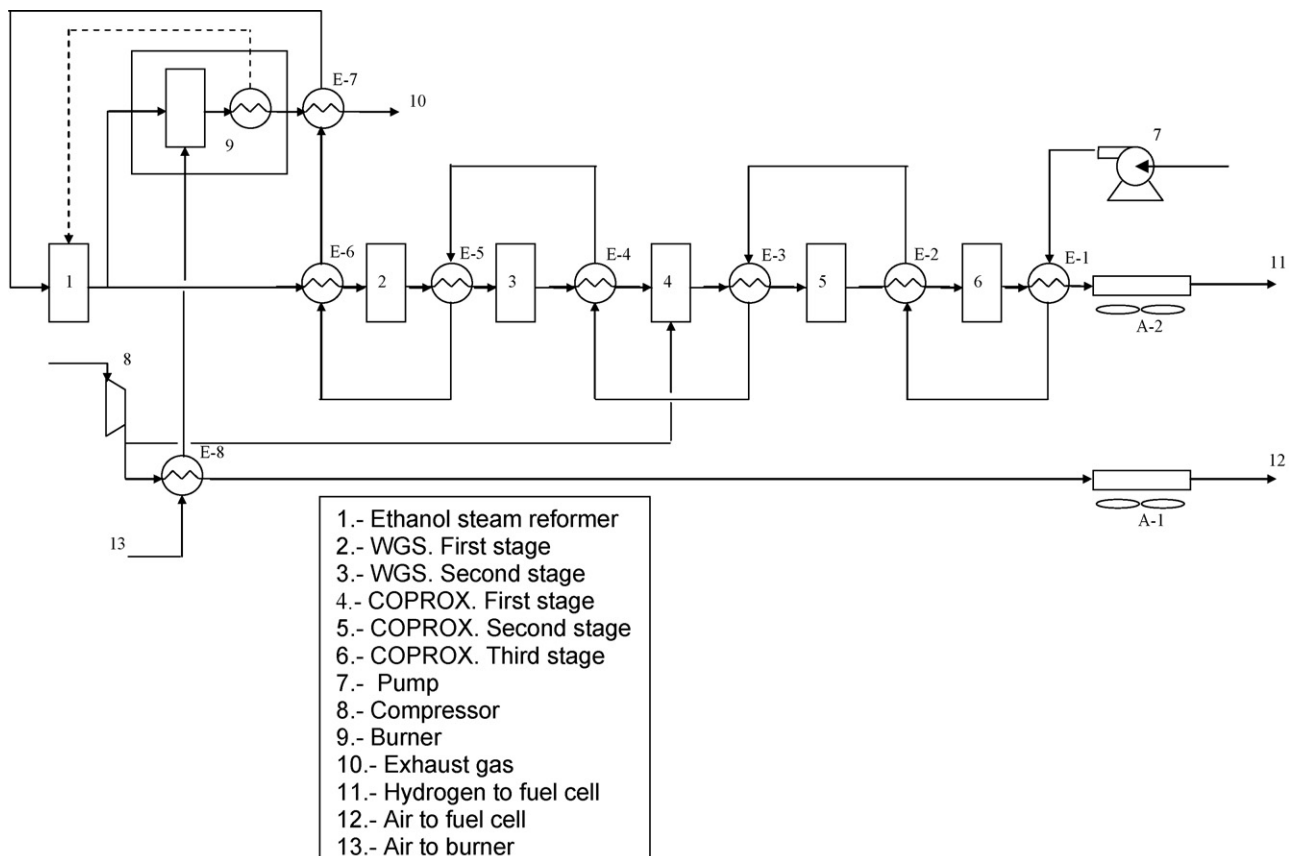

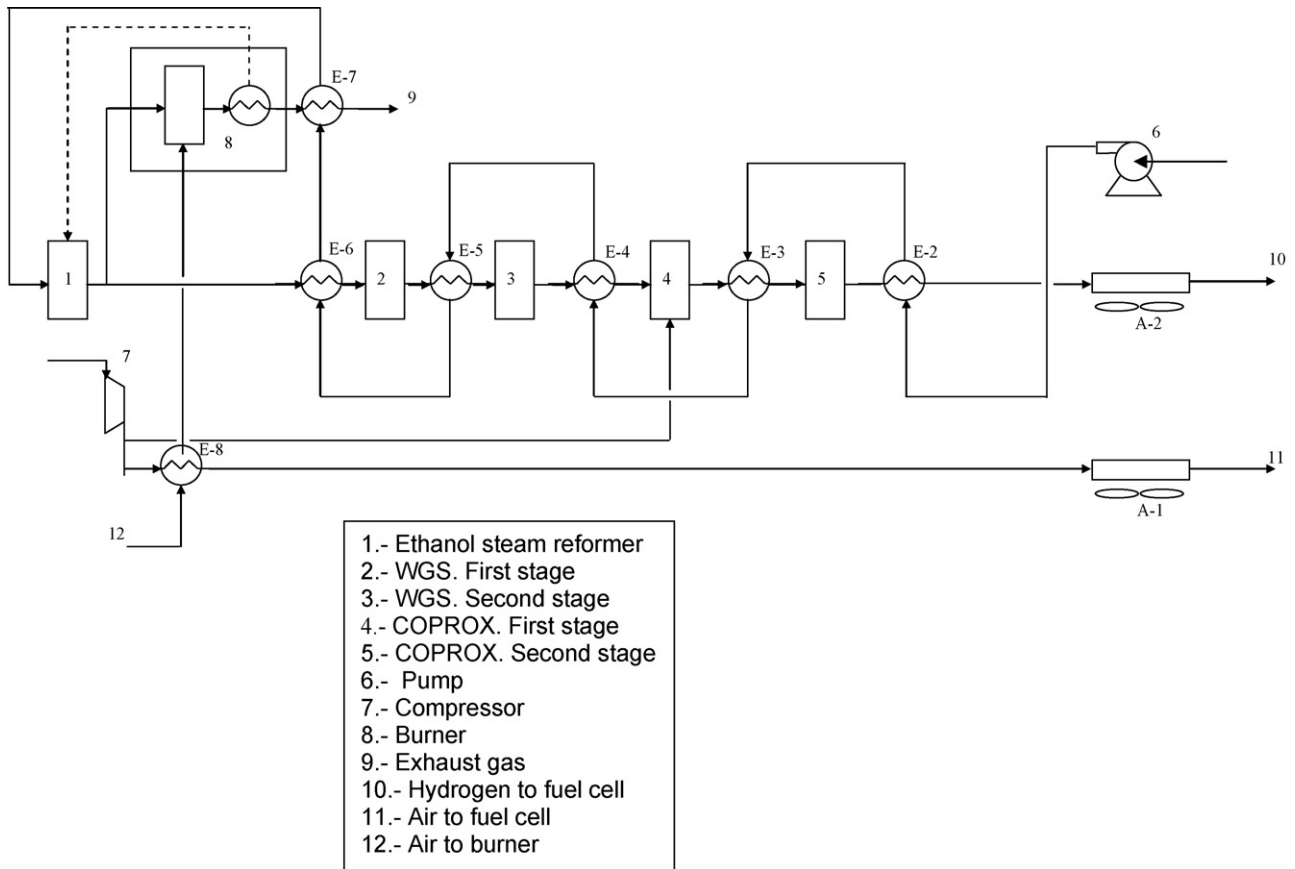Fig. 1. System flowsheet for $R \leq 1:4$ (Cases 1–10).

Fig. 2. System flowsheet for $R = 1:5$ (Cases 11–16).

1.- Ethanol steam reformer
2.- WGS. First stage
3.- WGS. Second stage
4.- COPROX. First stage
5.- COPROX. Second stage
6.- Pump
7.- Compressor
8.- Burner
9.- Exhaust gas
10.- Hydrogen to fuel cell
11.- Air to fuel cell
12.- Air to burner

question if the purpose is to reduce the volume of the entire device. However, as will be discussed later, the higher the temperature approach is, the lower the heat recovery will be. Thus, there is also a trade-off between system size and efficiency.

2.2.7. Air/fuel ratio in the burner

An adequate air/fuel ratio must produce a stream with enough heat content with a proper thermal level to keep temperature constant in the ESR. A low ratio implies deficient combustion and a high ratio leads to a lower thermal level.

2.2.8. Process stream fraction not burned

In order to minimize the burned process stream fraction, it would be necessary to choose the more adequate stream: ethanol, synthesis gas or hydrogen-rich stream. It is not the aim of this work to discuss which stream is the most convenient. Instead, synthesis gas is chosen for this purpose.

2.3. Heat exchanger network design

With the aim of minimizing the entropy difference and therefore maximize the useful work obtained, it is convenient that the heat exchange is carried out between two streams with temperatures which are not too different. Nevertheless, the closer the temperatures are, the larger the heat exchanger will be (see Section 2.2.6).

According to these considerations, the designs performed in this work are shown in Figs. 1–3, in which:

1. The cold stream start exchanging heat with hot streams of low thermal level before exchanging heat with hotter streams.
2. Since there is only one cold stream, it is divided into two in order to obtain two streams of lower thermal level.
3. The WGS and COPROX stages are divided each into two and three fixed beds, respectively, to exchange heat in order to limit the temperature increase.

3. Efficiency and power of the PEM fuel-cell

According to the First Principle of Thermodynamics, the following energy balance is considered:

$$W_e - W_b - W_c + Q_{FC} + Q_{A1} + Q_{A2}$$
$$= \sum_{inlet} F^i h^i - \sum_{outlet} F^i h^i = \Delta H_{sys} \quad (6)$$

where W_e is the electric power done by the system, W_b and W_c the power consumed by the pump and by the compressor, respectively, Q_{FC}, Q_{A1} and Q_{A2}, the heat exchanged in the fuel cell and air coolers A-1 and A-2 (see Figs. 1–3) with the environment, F^i the molar flow of the stream i, h^i its molar enthalpy and ΔH_{sys} is the difference in enthalpy flow rates, associated with the mass flow rates, at the overall system exit
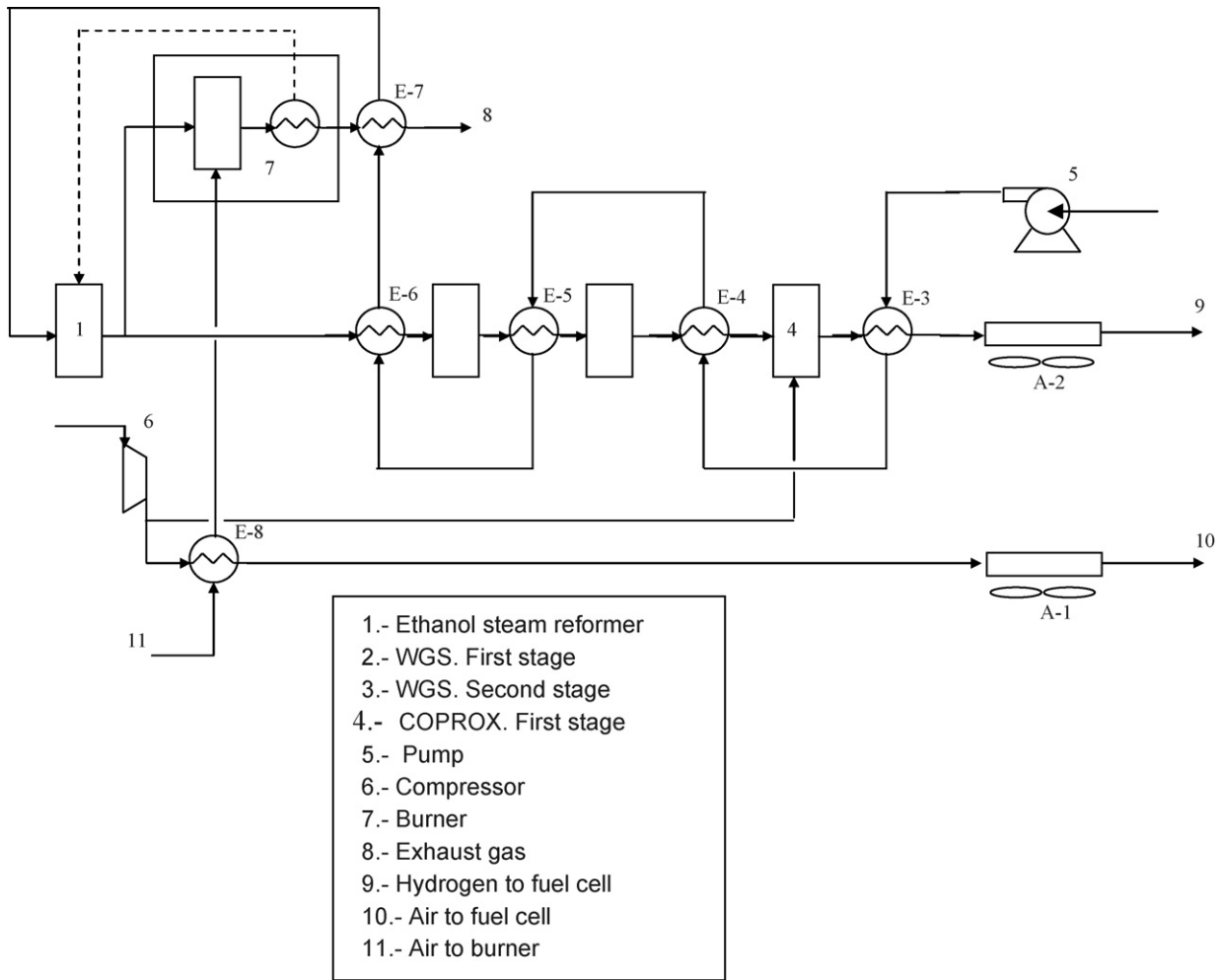
Fig. 3. System flowsheet for $R = 1{:}6$ (Cases 17–26).

and inlet planes. The electric power W_e is

$$W_e = I\Delta V = 2\text{Fa}\, F_{H_2} x_{H_2} \Delta V(I) \tag{7}$$

where I is the current intensity, $\Delta V(I)$ the fuel-cell differential of potential, Fa the Faraday constant ($96485\,\text{C}\,\text{mol}^{-1}$), F_{H_2} the hydrogen molar flow entering the fuel cell and x_{H_2} is the H_2 conversion in the first cell[1].

From Eqs. (6) and (7), the following expressions to evaluate the efficiency of the system (η) and the net power delivered, W_{net}, are proposed:

$$\eta_1 = \frac{W_{net}}{\sum_{inlet} F^i h^i - \sum_{outlet} F^i h^i} \times 100 = \frac{W_{net}}{\Delta H_{sys}} \times 100 \tag{8}$$

$$\eta_2 = \frac{W_{net}}{F_{etOH} \text{LHV}} \tag{9}$$

$$W_{net} = 2\text{Fa}\, F_{H_2} x_{H_2} \Delta V(I) - W_b - W_c \tag{10}$$

---

[1] For a stack of fuel cells electrically connected in series and also fed in series, the number of moles of H_2 reacted in each cell must remain constant, so as to obtain the same current intensity in the circuit which is generated at the first cell.

where LHV is the low heating value of the ethanol, $1.2355 \times 10^6\,\text{kJ}\,\text{kmol}^{-1}$.

As can be seen, it is possible to find an expression for the efficiency in terms of the First Principle (Eq. (8)) or in a way analogous to that of a thermal engine cycle (Eq. (9)). Both expressions have the net power generated in common.

In Eq. (8) the denominator accounts for the system enthalpy, while the denominator in Eq. (9) represents the amount of heat that the combustion of the entering ethanol would deliver.

The hydrogen flow in Eq. (10) is affected by: ESR temperature; process stream fraction not burned; inlet temperature in WGS and COPROX reactors; air/CO ratio in the COPROX reactor; ethanol/water feed ratio.

The differential of potential in the fuel cell is affected by some over potentials, namely:

- activation over-potential;
- limit current over-potential (mass transport over-potential);
- ohmic resistance over-potential.

Calculations are performed assuming that: (a) the sinks of power are the burner and the mechanical device and (b) the fuel cell can handle any amount of hydrogen.

In the present work, the actual tension value in the fuel cell was assumed as 0.5 V, based on Berning and Djilali [21].

4. Simulation

The simulation was performed under the following assumptions:

- No pressure drop is considered throughout the system.
- The compressor and pump adiabatic efficiencies are 75% each.
- The burner operates at atmospheric pressure and CO, CH_4 and H_2 combustion is complete.
- The air/synthesis gas molar flow ratio is 1.8.
- Room temperature: 20 °C.
- Inlet flow temperatures to the first stage of COPROX reactors are 180 °C.
- The conversion in the last stage of COPROX is adjusted to obtain a CO molar concentration lower than 20 ppm.
- The oxygen/CO molar feed ratio is 2.
- The hydrogen conversion in each COPROX reactor is 1% of the hydrogen stage inlet.
- Potential difference per cell: 0.5 V.
- The stack is capable of consuming any amount of hydrogen (i.e., $F_{H_2} = 0$ at the stack outlet).
- The oxygen/H_2 molar feed ratio is 0.5.

- The minimum temperature approach in any heat exchanger must be at least 25 °C.
- The air cooler fan power is not considered.
- No energy losses are considered.

The software employed was Aspen Hysys 3.1 [22], with which flow and enthalpy values were taken in order to compute the efficiency as well as the net power produced by the system.

Ethanol/water feed ratio and ethanol steam reformer temperature, two key variables in the energy integration, were analyzed. The most relevant results are shown in Table 1, where:

R	ethanol/water molar feed ratio
f	process stream fraction not burned
T_{REF}	ethanol steam reformer temperature [°C]
$T_{PROX,out}$	COPROX stage outlet temperature after heat exchange [°C]
T_{EX}	temperature of the burner exhaust gas [°C]
CO	CO concentration in the stream entering the fuel cell [ppm]
η	efficiency [%]
W_{net}	net power produced by the system [kW]

For $R \leq 1{:}3.6$, refer to Fig. 1. It must be noted that, in this case, air cooling (A-2) was not needed to achieve 80 °C in the hydrogen feed to the PEMFC. On the other hand, for $R > 1{:}4$, air cooling was needed (Figs. 2 and 3).

Table 1
Results of the simulation

Case	R	f	T_{REF}	$T_{PROX,out}$	T_{EX}	η_1	η_2	W_{net}
1	1:3.5	0.78	750	180	377.0	59.2	47.1	57.5
2	1:3.5	0.79	750	180	293.9	59.2	47.7	58.2
3	1:3.5	0.78	760	180	348.9	58.5	47.9	58.4
4	1:3.5	0.78	770	180	323.2	57.9	48.6	59.2
5	1:3.6	0.78	760	180	330.4	58.6	48.4	57.8
6	1:3.6	0.78	770	180	310.3	58.0	49.1	58.6
7[a]	1:4	0.76	760	85	330.7	58.9	49.0	53.8
8[a]	1:4	0.77	760	85	257.7	58.9	49.7	54.6
9[a]	1:4	0.76	770	85	306.7	58.2	49.5	54.4
10[a]	1:4	0.77	770	85	232.5	58.2	50.2	55.1
11[a,b]	1:5	0.70	760	95	361.7	61.1	50.2	46.0
12[a,b]	1:5	0.72	760	95	258.2	60.9	51.7	47.3
13[a,b]	1:5	0.73	760	95	199.6	60.8	52.4	47.9
14[a,b]	1:5	0.70	770	95	347.9	60.4	50.5	46.2
15[a,b]	1:5	0.72	770	95	242.9	60.3	51.9	47.5
16[a,b]	1:5	0.73	770	95	183.3	60.2	52.7	48.2
17[a,b,c]	1:6	0.66	760	100	334.0	64.6	52.4	41.1
18[a,b,c]	1:6	0.67	760	100	294.4	64.5	53.2	41.7
19[a,b,c]	1:6	0.68	760	100	251.5	64.4	54.0	42.4
20[a,b,c]	1:6	0.69	760	100	205.7	64.3	54.8	43.0
21[a,b,c]	1:6	0.66	770	100	325.1	64.0	52.6	41.2
22[a,b,c]	1:6	0.67	770	100	285.0	63.9	53.4	41.9
23[a,b,c]	1:6	0.68	770	100	241.8	63.8	54.2	42.5
24[a,b,c]	1:6	0.69	770	100	195.3	63.7	55.0	43.1
25[a,b,c]	1:6	0.69	790	100	179.1	62.9	55.2	43.3
26[a,b,c]	1:6	0.69	800	100	173.5	62.6	55.3	43.4

[a] Air cooling (A-2) employed to achieve 80 °C in the hydrogen-rich fuel-cell feed (Fig. 1).
[b] COPROX third stage is not needed to achieve [CO] < 20 ppm (Fig. 2).
[c] COPROX second stage is not needed to achieve [CO] < 20 ppm (Fig. 3).

Table 2
Heat exchange

	Q [kW]	ΔT_{min} [°C]
E-1	4.523	35.95
E-2	1.479	50.24
E-3	1.483	45.18
E-4	1.386	44.60
E-5	1.479	38.18
E-6	12.14	43.00
E-7	14.21	39.17
E-8	1.873	25.00
A-1	2.200	–
A-2	0.686	–

For $R \geq 1{:}5$ (Fig. 2), the third stage of the COPROX reactor was no longer needed, since the CO depletion in the ESR and the WGSR was more complete. Thus, this third bed and the heat exchanger which is downstream (E-1) were eliminated.

For $R \geq 1{:}6$ (Fig. 3), the second stage of the COPROX, together with the exchanger E was also eliminated for the same reasons stated above.

Table 2 shows the values of the heat exchanged in each device for Case 10, where E represents a device in which two streams exchange heat, and A, a device in which a single stream exchanges heat with the environment (air cooler). For further details, refer to Figs. 1–3.

5. Discussion and conclusions

In this work, the feasibility to carry out the energy integration for the hydrogen catalytic production and purification—PEM fuel-cell, using ethanol as raw material was demonstrated, with efficiencies η_1 ranging 57–64% and η_2 ranging 47–56%. These efficiencies should be taken as a ceiling, since the working efficiency must include energy losses (heat loss in tubing or reformer furnace, Joule effect, electrical motor intrinsic efficiency, excess of any material stream, etc.).

It can be noted that for all of the cases analyzed the efficiencies obtained are higher than those of internal combustion engines with the additional advantage that CO_2 concentration in the atmosphere is not increased.

The efficiency is affected by the number of heat exchangers and by the minimum temperature approach. A large number of heat exchanges allows a more efficient heat recovery, and thus more power is available. Concerning the minimum temperature approach, low differences also allow a better heat integration. Nevertheless, both alternatives have the penalty of a higher required volume. Thus, if this system is to be included in a vehicle, the restriction in the system volume shall lead to a reduction in the overall efficiency.

Despite this fact, it is possible obtain a sustainable system burning about 20–34% of the ethanol steam reformer effluent. That is, it is possible to develop a system in which the inputs are ethanol, water and air and the outputs are electricity, heat and basically CO_2 and water.

The operational conditions of the WGSR and COPROX (performing a heat exchange between each catalytic bed) are closer to the evolutions of those corresponding to equilibrium (reversible), thus reducing the entropy of the system and increasing the availability of the energy to obtain useful work.

High temperatures in the ethanol steam reformer increase the efficiency and the power because methane yield is lowered at these conditions. Besides, in this stage, when possible, higher temperatures imply a better heat recovery of the exhaust gases (see Table 2).

Fuel-cell power decreases for increasing R since more energy is required to evaporate the water entering the ethanol steam reformer. Nevertheless, $|\Delta H_{sys}|$ also decreases in such a way that η_1 increases (see Eq. (8)). A rise in η_2 can be noticed as well, since an increment in R implies a diminution in ethanol feed flow (see Eq. (9)).

It must be noted that f decreases when R decreases for the same reason stated above, i.e., more energy is required, and this energy is obtained from burning part of the outlet of the reformer stage.

At constant R, W_{net} increases with T_{REF}, and so does η_2 (the denominator in Eq. (9) remains constant). However, $|\Delta H_{sys}|$ also increases, since a rise in T_{REF} has the effect of recovering heat from the burner exhaust gases (see Table 1). Thus, a drop in η_1 is observed.

The results shown in this work, as well as those obtained in previous papers [3,5,11,17,20] indicate that the technology of fuel-cell grade hydrogen production using ethanol as raw material is a very attractive alternative to those technologies based on fossil fuels.

References

[1] V. Klouz, V. Fierro, P. Denton, H. Katz, J.P. Lisse, S. Bouvot-Mauduit, C. Mirodatos, J. Power Sources 4549 (2001) 1–9.
[2] L.F. Brown, Int. J. Hydrogen Energy 26 (2001) 381–397.
[3] F.J. Mariño, M. Boveri, G. Baronetti, M. Laborde, Int. J. Hydrogen Energy 26 (7/2001) 665–668.
[4] F. Auprêtre, C. Descorme, D. Duprez, Catal. Commun. 3 (2002) 263–267.
[5] J. Comas, F. Mariño, M. Laborde, N. Amadeo, Chem. Eng. J. 98 (2004) 61–68.
[6] A.N. Fatsikostas, X.E. Verykios, J. Catal. 225 (2004) 439–452.
[7] E.Y. Garcia, M.A. Laborde, Int. J. Hydrogen Energy 16 (5) (1991) 307–312.
[8] V. Mas, R. Kipreos, N. Amadeo, M. Laborde, Int. J Hydrogen Energy 31 (1) (2006) 21–28.
[9] J.M. Zalc, D.G. Löffler, J. Power Sources 111 (2002) 58–64.
[10] J. Sun, X. Qiu, F. Wu, W. Zhu, Int. J. Hydrogen Energy 30 (2005) 437–445.
[11] J. Comas, V. Mas, G. Baronetti, M. Laborde, N. Amadeo, Hypothesis VI, vol. 1, La Habana, Cuba, May 8–12, 2005, pp. 277–283.
[12] S. Freni, J. Power Sources 94 (2001) 14–19.
[13] J. Viñas, G. Barreto, M. González, M. Laborde, N. Moreno, LAR 1999 29 (2) (1999) 91–98.
[14] N. Amadeo, M. Laborde, Int. J. Hydrogen Energy 20 (12) (1995) 949–956.
[15] M. Ginés, N. Amadeo, M. Laborde, C. Apesteguía, Appl. Catal. A: Gen. 131 (1995) 283–296.
[16] N. Amadeo, M. Laborde, Trends Chem. Eng. 3 (1996) 159–183.

[17] P. Giunta, N. Amadeo, M. Laborde, J. Power Sources 156 (2006) 489–496.

[18] F. Mariño, C. Descorme, D. Duprez, Appl. Catal. B: Environ. 54 (2004) 59–66.

[19] F. Mariño, C. Descorme, D. Duprez, Appl. Catal. B: Environ. 58 (2005) 175–183.

[20] S. Larrondo, J. Comas, G. Alvaro, B. Schönbrod, F. Mariño, M. Laborde, N. Amadeo, XIX Simposio Iberoamericano de Catálisis, Mérida, México, September 5–11, 2004, 2004, pp. 1175–1182 (CD version).

[21] T. Berning, N. Djilali, J. Power Sources 124 (2003) 440–452.

[22] http://www.hyprotech.com, accessed August 2006.